Environmental Science Nano

PAPER

View Article Online
View Journal | View Issue

Cite this: *Environ. Sci.: Nano*, 2016, **3**, 418

Impact of chemical composition of ecotoxicological test media on the stability and aggregation status of silver nanoparticles†‡

George Metreveli,[a] Bianca Frombold,[a] Frank Seitz,[b] Alexandra Grün,[c] Allan Philippe,[a] Ricki R. Rosenfeldt,[b] Mirco Bundschuh,[bd] Ralf Schulz,[b] Werner Manz[c] and Gabriele E. Schaumann*[a]

Received 11th July 2015,
Accepted 8th January 2016

DOI: 10.1039/c5en00152h

rsc.li/es-nano

Understanding of the interplay of generally known colloidal transformations under conditions of test media (TM) used during cultivation of organisms and biological effect (=ecotoxicological) studies is still limited, although this knowledge is required for an adequate interpretation of test outcomes and for a comparison among different studies. In this context, we investigated the aggregation and dissolution dynamics of citrate-stabilized silver nanoparticles (Ag NPs) by varying the composition of three TM (ASTM, SAM-5S, and R2A, used during bioassays with *Daphnia magna*, *Gammarus fossarum*, and bacterial biofilms, respectively) in the presence and absence of two types of natural organic matter (NOM), namely, Suwanee River humic acid (SRHA) and seaweed extract (SW). Each original test medium induced reaction-limited aggregation of Ag NPs, and aggregation increased from R2A to SAM-5S and ASTM. In addition to the differences in aggregation dynamics, the concentration and speciation of Ag(I) differed between the three TM, whereby SAM-5S and ASTM are comparable with respect to the nature of the aggregation process but clearly differ from the R2A medium. Furthermore, Cl^-, mainly present in SAM-5S, induced NP stabilization. The release of silver ions from Ag NPs was controlled by the presence of NOM and organic constituents of TM and by interactions with Cl^- and Br^-. The degree of aggregation, formation of interparticle cation–NOM bridges or stabilization was larger for Ca^{2+} than for Mg^{2+} due to the stronger ability of Ca^{2+} to interact with citrate or NOM compared to Mg^{2+}. These observations and the dependence of aggregation rates on the particle concentration renders the interpretation of dose–response relationships challenging, but they may open perspectives for targeted ecotoxicological testing by modifications of TM composition.

Nano impact

Ecotoxicological studies on engineered nanoparticles (NPs) are conducted involving different test media (TM), whose composition is adapted towards the needs of the respective species. This composition significantly influences the colloidal state and properties of NPs. In this work, the aggregation and dissolution dynamics of Ag NPs were characterized in three different TM by varying their composition. The dissolution of Ag NPs was controlled by surface protection by natural organic matter (NOM) and organic constituents of TM and by interactions with Cl^- and Br^-. In general, reaction-limited aggregation was observed. Aggregation depended predominantly on the Ca^{2+}/Mg^{2+} ratio, anion composition and NOM quality. This knowledge will support the interpretation of and comparison among ecotoxicological studies that may have been performed under differing conditions.

[a] *Group of Environmental and Soil Chemistry, Institute for Environmental Sciences, University of Koblenz-Landau, Fortstrasse 7, D-76829 Landau, Germany. E-mail: schaumann@uni-landau.de*
[b] *Group of Ecotoxicology and Environment, Institute for Environmental Sciences, University of Koblenz-Landau, Fortstrasse 7, D-76829 Landau, Germany*
[c] *Department of Biology, Institute of Integrated Natural Sciences, University of Koblenz-Landau, Universitätsstrasse 1, D-56070 Koblenz, Germany*
[d] *Department of Aquatic Sciences and Assessment, Swedish University of Agricultural Sciences, Lennart Hjelms väg 9, SWE-75007 Uppsala, Sweden*

† The authors declare no competing financial interest.

‡ Electronic supplementary information (ESI) available: Details of the Ag NP synthesis method; preparation method of SRHA stock solution; calculation of centrifugation duration; chemical composition of TM; pH values in TM after the addition of NOM and Ag NP; chemical composition of the stock solutions used for early stage aggregation experiments; input parameters used in the model calculations; speciation of silver in TM; metal concentrations in organic compounds used for preparation of R2A; particle size distribution (DLS) and TEM images of Ag NP; hydrodynamic diameter of Ag NP in TM for the first 60 min as a function of exposure time; hydrodynamic diameter of Ag NP in ASTM and R2A at different particle concentrations; initial aggregation rates of 30 nm Ag NP in modified ASTM medium in the absence and presence of vitamins (B_1, B_7 and B_{12}); initial aggregation rates of 30 nm Ag NP in deionized water in the presence of 0.03 mmol L^{-1} Ca^{2+} and at different Na^+ concentrations; initial aggregation rates of 30 nm Ag NP in deionized water and in Mg^{2+}-free R2A medium in the absence and presence of individual organic constituents of R2A and their mixtures. See DOI: 10.1039/c5en00152h

Introduction

Assessing the potential environmental impact of engineered nanoparticles (NPs) frequently involves the use of well-defined test media (TM). Their composition has been carefully adapted towards the specific needs of the test organisms of interest. The different ionic and molecular backgrounds of the multitude of applied TM necessarily lead to a variety of NP transformations based on aggregation (in order to cover strongly as well as weakly bound NP clusters expected in TM, we use only the term "aggregation" regardless of the type of particle clusters), coating by TM constituents and interactions with organic matter (OM). Such transformations may affect the ecotoxicological potential of NPs[1] and thus lead to TM-dependent biological responses. This may, at least partly, explain discrepancies of ecotoxicological effect thresholds among studies. Despite this relevance, only limited information is available on potential NP transformations in TM up to now.

It is known that the typically high ionic strength in TM promotes the aggregation of silver,[2–5] gold,[6] titanium dioxide,[1,7–9] zinc oxide,[7,10] and cerium dioxide[11] NPs. Also, general impacts of individual TM constituents and additives (*e.g.*, halides,[12–16] multivalent cations,[17–20] suspended minerals,[21] natural organic matter (NOM)[21,22]) on NP transformations are well known from lab studies in well-defined systems. Some studies specifically focused on the role of individual TM constituents or additives in complex systems: Nur *et al.*[9] observed that titanium dioxide NPs aggregated according to the classical Derjaguin–Landau–Verwey–Overbeek (DLVO) theory despite the complex chemical composition of the test media. The critical coagulation concentration (CCC) of TM for titanium dioxide NPs as determined by diluting the TM varied between 18% and 54%,[9] which indicates that aggregation of these NPs in the original (100%) TM is diffusion limited. The dilution of TM in order to obtain stable Ag NP dispersions was also applied in other studies and suggested that dilution by a factor of 10 would reduce aggregation sufficiently for the tests.[2–4] Tejamaya *et al.*[4] reported increased shape and dissolution changes for citrate-coated Ag NPs after replacement of Cl^- by SO_4^{2-} and NO_3^-. Horst *et al.*[8] observed the stabilizing effect of humic acid (HA) on titanium dioxide NPs in TM. Besides these findings, it is still largely unknown which of the generally known fundamental colloidal processes dominate NP transformation in which TM, to which extent the NP status varies among TM, and which aggregation mechanisms are relevant under which conditions. This knowledge is of high importance as the type of aggregation mechanism will influence, among others, how strongly the NP status is governed by NP concentration and how the type of coating and the tendency for dissolution are expected to affect the ecotoxicological potential of NPs.

From systems containing a lower variety of constituents than most TM, it is known that besides the ionic strength, the type of cations and anions is important for the aggregation of NPs. Divalent cations show higher efficiency to induce aggregation than monovalent cations.[17–20] Furthermore, aggregation of citrate-coated Ag NPs is more pronounced in the presence of Ca^{2+} compared to Mg^{2+}, which may be explained by the higher ability of Ca^{2+} to form complexes with citrate.[14,18] Thus, not only differences in the total concentration of divalent cations but also differences in the molar ratio of Ca^{2+} and Mg^{2+} in TM will result in different aggregation states and, thus, different ecotoxicological responses. Furthermore, TM composition differs with respect to the presence and absence of halide ions. Chloride, for example, may either enhance or suppress the aggregation of Ag NPs. Ag NP stabilization by the formation of negatively charged AgCl(s) precipitates on the NP surface was observed in several studies,[4,12,13] whereas Baalousha *et al.*[14] reported enhanced aggregation due to interparticle bridging by solid phase AgCl(s).

Even more complex is the role of organic substances in the TM. Depending on the needs of the target organisms, TM contain various organic substances (proteins, enzymes, vitamins, glucose and others) at variable concentrations. Their role for the NP transformation in TM still requires investigation. Furthermore, NOM is increasingly used as an NP-stabilizing additive to traditional TM.[1,8] However, NOM can induce either stabilization or destabilization of NPs, depending on the solution chemistry and the type of NOM used.[22] Especially, the interplay between bridging-determined aggregation, which is observed predominantly at a high concentration of multivalent cations,[14,18,23–25] and electrosteric stabilization[23,26,27] will depend strongly on the quality of the NOM and on the concentration as well as types of multivalent cations. As reported by Stankus *et al.*,[24] Mg^{2+} induced the bridging-determined aggregation to a lower extent compared to Ca^{2+}. As TM normally contain a mixture of salts and sometimes various NOM additives, it will be essential to understand the combined effects of NOM and all cations as well as their individual contributions to the transformation of NPs. Special emphasis has to be put on differences between Mg^{2+} and Ca^{2+} and between NOM types and their ability to interact with these multivalent cations. Moreover, the suggested impeding impact of NOM on the Ag NP dissolution[28–30] seems to be highly relevant for ecotoxicological testing.[31] However, to date, no study is available in which the TM composition was varied systematically in order to elucidate the underlying NP transformation mechanisms and identify dominating effects.

Furthermore, the concentration of NPs influences their transformations in TM. For high NP concentrations (from 50 to 500 mg L^{-1}) as used in some ecotoxicological studies,[7,8,10,11] aggregation is significantly accelerated.[32–34] Thus, dose–response relationships[7,35,36] may be further distorted by NP concentration-dependent dynamics in aggregation during the tests. Moreover, the concentration of NPs available for the organisms can be changed by sedimentation of aggregated NPs. This can additionally complicate the interpretation of ecotoxicological test results.[37]

On the example of silver nanoparticles (Ag NPs), which are widely used in consumer products, the central aim of this

study was to elucidate how and to which extent individual TM constituents trigger specific NP transformations and which mechanisms are responsible for these processes. In particular, we tested the following hypotheses. i) Aggregation of Ag NPs in TM without NOM and other organic compounds is described by the classical DLVO theory and it is predominantly determined by the concentration of Ca^{2+}. ii) The presence of halide ions or organic compounds in TM modifies the NP surface, but NP aggregation is still dominated by the concentration of Ca^{2+}. iii) Under the conditions of different TM, the NOM generally suppresses aggregation *via* electrosteric stabilization and hinders Ag NP dissolution. iv) NP size does not alter the aggregation mechanism. v) For NOM that interact strongly with Ca^{2+}, there is a threshold value of Ca^{2+} concentration above which electrosteric stabilization is overlaid by bridging-determined aggregation.

In order to evaluate these hypotheses, the aggregation dynamics of citrate-stabilized Ag NPs was investigated in three TM: ASTM, SAM-5S, and R2A used during bioassays with *Daphnia magna*, *Gammarus fossarum*, and bacteria, respectively. In order to obtain process-based understanding, we characterized the influence of NOM, the cations Ca^{2+} and Mg^{2+}, and the anions Cl^-, Br^-, SO_4^{2-}, and NO_3^- as well as the concentration of NPs on the aggregation of Ag NPs by systematic variation of the TM chemical composition. In order to understand the influence of the particle size on the NP transformations under TM conditions, we used NPs in two different sizes (*i.e.*, 30 nm and 100 nm). Furthermore, the release of silver from Ag NPs was investigated in the presence as well as in the absence of NOM.

Materials and methods

Deionized water (resistivity: 18.2 MΩ·cm, Direct-Q UV, Millipore) was used for sample preparation in all experiments.

Silver nanoparticles

Ag NPs (30 nm and 100 nm) were synthesized by a citrate reduction method modified from Turkevich *et al.*[38] (for details see the ESI‡). The hydrodynamic diameter of Ag NP was measured *via* dynamic light scattering (DLS) at a scattering angle of 165° and the zeta potential was determined *via* an electrophoretic light scattering technique and was calculated using the Smoluchowski equation[39] (both using Delsa Nano C, Beckman Coulter). In the aggregation experiments the zeta potential was measured 5 min after adding Ag NPs to the TM. Due to the relatively low sensitivity of the electrophoretic light scattering at reduced particle number concentrations, which is expected in response to the aggregation over time, the zeta potential was not measured for longer exposure durations. Nanoparticles were additionally characterized by transmission electron microscopy (TEM; LEO 922 Omega, ZEISS) after nebulization of the suspensions using an ultrasonic generator onto a 3 mm copper grid covered with a combined holey and ultrathin (about 3 nm) carbon film (Ted Pella, Inc.).

Preparation of TM

ASTM medium (used during bioassays with *Daphnia magna*),[40,41] SAM-5S medium (used during bioassays with *Gammarus fossarum*),[42] and R2A medium (used during cultivation of bacteria and conducting of biofilm bioassays) were prepared as outlined in Table S1–S3.‡ ASTM contains vitamins, 0.107 mmol L^{-1} Cl^-, and in total 1.7 mmol L^{-1} Ca^{2+} plus Mg^{2+}; SAM-5S medium is free of organic compounds and contains 2.051 mmol L^{-1} Cl^-, 0.01 mmol L^{-1} Br^-, and 1.25 mmol L^{-1} Ca^{2+} plus Mg^{2+}; and R2A contains in total 0.2 mmol L^{-1} Mg^{2+} and various OM as well as Tween 80 (Table S4‡).

The TM were, if needed, amended with NOM as follows: Suwannee River HA (SRHA) standard II from the International Humic Substance Society (for the preparation method for SRHA stock solution, see the ESI‡) was used as the model NOM. Additionally, seaweed extract (SW; Marinure®) from Glenside was used in experiments with ASTM due to its frequent use in ecotoxicological testing.[37,43,44] The total organic carbon (TOC) concentration was adjusted to 9.4 mg L^{-1} SRHA and 8.0 mg L^{-1} SW, corresponding to the total mass concentration of 20 mg L^{-1} for both NOM. Whereas SRHA contains carboxylic and phenolic functional groups, SW contains polysaccharides with hydroxyl, carboxylic, and amino functional groups;[45] thus the two NOM are expected to have a different affinity to multivalent cations. Following the categorization of NOM into NOM of aquatic origin and of rather terrestrial origin,[46] it may be postulated from their composition that SW is likely to resemble aquatic NOM, while SRHA rather resembles NOM of terrestrial origin, the latter due to its higher affinity to Ca^{2+}.[47]

In order to measure the concentration of metals in R2A medium, potentially originating not only from Na-pyruvate but also from other individual organic compounds, the solutions of each individual organic compound were prepared at the same concentration as that used in R2A medium. Metal concentration was measured in unfiltered and with 3 kDa membrane (Amicon Ultra-15 centrifugal filter device, Merck Millipore) filtered solutions using an inductively coupled plasma optical emission spectrometer (ICP-OES, 720, Agilent Technologies).

Ag^+ release

Due to the higher specific surface and expected higher dissolution rate, Ag^+ release from Ag NPs was investigated in batch experiments exemplary for 30 nm Ag NPs in the absence and presence of the respective NOM. The Ag NP stock dispersion, NOM stock solution and medium were introduced into 50 mL polypropylene centrifuge tubes (VWR). The concentration of Ag NP was set to 2 mg L^{-1}, which approximates the mean value of the broad concentration range used in ecotoxicological studies. All samples were prepared in triplicate. After shaking for 1 and 7 days using a laboratory shaker at 20 rpm (rotation angle: 180°, INTELLI-MIXER, NeoLab), two 8.5 mL aliquots from each sample were distributed in two

ultracentrifuge tubes (polycarbonate) and centrifuged at 396 000*g* for 2 h (SORVALL WX 90 Ultra, Thermo Electron Corporation). This allows separation of Ag NPs (cutoff: 2 nm) from the supernatant (ESI‡), which contains Ag^+ and, if present, ultra-small Ag NPs (<2 nm). This fraction is abbreviated as $Ag_{<2nm}$ in the following. After centrifugation, 5 mL of the supernatant was removed from each tube. Supernatants from two aliquot samples were recombined in one 15 mL centrifuge tube (Polypropylene, VWR) to obtain a sufficient volume (10 mL) for the subsequent analysis. The Ag concentration in the supernatant was finally determined by inductively coupled plasma mass spectrometry (ICP-MS, XSeries 2, Thermo Scientific) after acidification with 100 μL of 65% HNO_3 (sub-boiled). The concentration of $Ag_{<2nm}$ in undiluted Ag NP stock dispersion was also determined.

Model calculations for Ag(I) species

In order to be able to compare our results with information about the distribution of thermodynamically expected Ag(I) species in TM, the speciation calculation was done for $Ag_{<2nm}$ concentrations detected in Ag^+ release experiments with 1 d shaking duration using Visual MINTEQ software version 3.0.[48] The calculations were performed based on the assumption that the $Ag_{<2nm}$ fraction in ultracentrifuged samples solely represents dissolved Ag(I) species. Ag(I) speciation was calculated for a CO_2 equilibrium between air and the aqueous phase. The input parameters used in the model calculations are presented in Table S9.‡

Long-term aggregation

Long-term aggregation was investigated for 30 nm and 100 nm Ag NPs in all TM in the absence and presence of the respective NOM. Therefore, Ag NP stock dispersion was added to the TM directly in the size measurement cuvette (total sample volume: 3 mL; Ag NP concentration 2 mg L^{-1}). The pH values are listed in Table S5‡ and were not significantly influenced by NOM and Ag NPs. Samples were manually shaken for 2–3 s. The *Z*-average hydrodynamic diameter was measured for the first 60 min every 42 s as well as after 1 d and 7 d covering the typical duration of some toxicity tests, for example, those performed with *Gammarus fossarum*.[41,49] As a control, the particle size of Ag NPs was measured in deionized water at the same particle concentration over the same test duration. All experiments were performed in duplicate.

Early-stage aggregation kinetics

Early-stage aggregation kinetics were investigated for 30 nm Ag NPs (concentration 2 mg L^{-1}) in the absence and presence of NOM in all TM but varying the Ca^{2+} (as $CaSO_4$) or Mg^{2+} (as $MgSO_4$) concentration (0.1–12 mmol L^{-1}). For this, stock solutions of salts and organic compounds (Table S6–S8‡) were prepared. The previously calculated volume of deionized water and stock solutions was added directly into the size measurement cuvette. The samples prepared for Ca^{2+} and Mg^{2+} addition did not contain Mg^{2+} and Ca^{2+} ions, respectively. Furthermore, the ionic strength-dependent aggregation kinetics of Ag NP were investigated in mixtures of Ca^{2+} and Mg^{2+} at the Ca^{2+}/Mg^{2+} molar ratios of 0.7/1 and 1/0.25 as used in ASTM and SAM-5S, respectively. DLS measurements were conducted for the first 10 min every 30 s, starting 30 s after the addition of Ag NPs. The resulting pH values are shown in Table S5.‡ All experiments were duplicated.

In order to elucidate the influence of vitamins on the aggregation of Ag NPs in TM, early-stage aggregation experiments were performed for 30 nm Ag NPs in the absence and presence of $CaSO_4$ (0.7 mmol L^{-1}) in modified ASTM medium, which contained vitamins at different concentrations (B_1: 0.075, 0.5, 5 mg L^{-1}; B_7: 0.00075, 0.005, 0.05 mg L^{-1}; B_{12}: 0.001, 0.01, 0.1 mg L^{-1}). To exclude the influence of Mg^{2+} on the aggregation, the modified ASTM medium did not contain Mg^{2+} ions. To investigate the role of inorganic anions in the aggregation of Ag NPs, early-stage aggregation experiments were done for 30 nm Ag NPs in deionized water and modified ASTM medium in the absence and presence of $CaSO_4$ (for manufacturer and purity, see Table S1‡), $CaCl_2$ (for manufacturer and purity, see Table S2‡), $Ca(NO_3)_2{\cdot}4H_2O$ (≥99%, *p.a.*, Carl Roth), or $CaBr_2$ (99.5%, Alfa Aesar) at the same Ca^{2+} concentration (0.7 mmol L^{-1}). The modified ASTM medium did not contain Mg^{2+} ions and vitamins to exclude their influence on the aggregation. In order to test the influence of monovalent cations on the aggregation of Ag NPs in R2A medium, early-stage aggregation experiments were performed in deionized water at the same divalent cation concentration as detected in R2A medium (0.03 mmol L^{-1} Ca^{2+} as $Ca(NO_3)_2$, Table S12‡) and at different $NaNO_3$ (≥99%, *p.a.*, Carl Roth) concentrations (0–60 mmol L^{-1}). In order to elucidate the role of the individual organic constituents of R2A on the aggregation of Ag NPs (30 nm), early-stage aggregation experiments were done in Mg^{2+}-free R2A medium in the absence and presence of individual organic constituents and their mixtures at the same concentrations as present in the medium. In addition, the influence of NP concentration on the aggregation pattern was investigated exemplarily in the NOM-free ASTM medium for particle concentration ranges of 0.1–10 mg L^{-1} (30 nm NP) and 1–10 mg L^{-1} (100 nm NP) as well as in Mg^{2+}-free R2A medium for the particle concentration range of 0.5–10 mg L^{-1} (30 nm NP).

Evaluation of aggregation kinetics

The aggregation rate constant, k, is proportional to the initial change in the hydrodynamic diameter of the nanoparticles, D_{NP}, with time and inversely proportional to the initial particle concentration N_0 in the early aggregation stage:[17,18]

$$k \propto \frac{1}{N_0}\left(\frac{\mathrm{d}\,D_{NP}(t)}{\mathrm{d}\,t}\right)_{t\to 0} \quad (1)$$

$(\mathrm{d}D_{NP}(t)/\mathrm{d}t)_{t\to 0}$ was determined by linear regression[17,18] for the first 180 s.

The attachment efficiency, α, was calculated by normalizing the aggregation rate constant of interest to the aggregation rate constant obtained for the diffusion-limited aggregation regime (k_{fast}):[17,18]

$$\alpha = \frac{1}{W} = \frac{k}{k_{fast}} = \frac{\frac{1}{N_0}\left(\frac{dD_{NP}(t)}{dt}\right)_{t\to 0}}{\frac{1}{(N_0)_{fast}}\left(\frac{dD_{NP}(t)}{dt}\right)_{t\to 0,fast}}, \quad (2)$$

W is the stability ratio and k_{fast} is independent of the electrolyte concentration.[17,18] The value of k_{fast} was obtained as a mean value of the aggregation rate constants at cation concentrations where no significant concentration dependency of aggregation rate constants was observed anymore. Thus, for nanoparticles aggregating due to classical DLVO interactions[50,51] (*e.g.*, in the absence of NOM) α will increase from zero to one. α <1 indicates reaction-limited aggregation, while α = 1 indicates diffusion limitation. α in the presence of NOM was calculated by normalizing k in the presence of NOM to k_{fast} in the absence of NOM. α >1 indicates additional aggregation mechanisms (*e.g.*, interparticle bridging).[25] The CCC was determined from the intersection of linear fitting functions of α under reaction- and diffusion-limited regimes in double-logarithmic scale.[25]

Results and discussion

Ag NP characteristics

Ag NPs were predominantly spherical; 20% (30 nm Ag NP) and 7% (100 nm Ag NP) were present as rods and triangles, respectively (Fig. S1‡). DLS indicated a *z*-average hydrodynamic diameter of 31.2 ± 1.2 nm and 107.3 ± 1.9 nm and a polydispersity index of 0.37 ± 0.03 and 0.18 ± 0.03 (mean ± standard deviation, n = 3) for the 30 nm and 100 nm Ag NPs, respectively. Since the number weighting shifts much stronger the particle size distribution to the small particle sizes than volume weighting,[52] the volume weighted median particle diameter was calculated from TEM data in order to validate the DLS results. The volume weighted median particle diameter obtained from TEM images under the assumption that all particles are spherical was 67 nm (30 nm Ag NPs) and 95 nm (100 nm Ag NPs). The differences in size obtained by DLS and TEM especially for 30 nm Ag NPs is due to size and shape polydispersity which may have induced a systematic error in the determination of the average hydrodynamic diameter by DLS.[53,54] Also, the presence of non-spherically shaped NPs as observed by TEM may have introduced some uncertainties during the data evaluation due to the assumption of spherical shape for all particles. More detailed information on the particle size distribution of 30 nm Ag NPs can be found in Metreveli *et al.*[23] The Ag NPs revealed zeta potentials of -59.4 ± 1.6 mV and -58.9 ± 0.5 mV (mean ± standard deviation, n = 3) for 30 nm and 100 nm Ag NPs, respectively. The highly negative zeta potential underlines the high stability (>1 year) of both Ag NP dispersions.

Ag^+ release

In all experiments, the concentration of $Ag_{<2nm}$ was higher than the initial $Ag_{<2nm}$ concentration (1.1 ± 0.5 μg L^{-1}; Fig. 1) and differed among the TM, which suggests significant and TM-dependent dissolution of Ag NPs. In the absence of NOM, 5.2%, 0.5% and 0.1% of the initially spiked 2 mg L^{-1} total silver was released in ASTM, SAM-5S and R2A, respectively, resulting in $Ag_{<2nm}$ concentrations after one day from 3.9 ± 2.2 μg L^{-1} (R2A) to 105.6 ± 0.4 μg L^{-1} (ASTM). One possible explanation for the differences among TM might be their substantial difference in terms of Cl^- concentration (107 μmol L^{-1} in ASTM, 2051 μmol L^{-1} in SAM-5S and 0 μmol L^{-1} in R2A). Furthermore, SAM-5S contains Br^- (10 μmol L^{-1}), which is not present in ASTM and R2A medium and undergoes even stronger interactions with Ag(I), such that an impact of Br^- even at this low concentration cannot be excluded.

As reported in the literature, the dissolution and ecotoxicological impact of Ag NPs is strongly affected by the Cl^- concentration.[15,16] Furthermore, the different conditions in the TM will lead to TM-dependent Ag speciation and therefore to potentially different impacts on the Ag NP status. Model calculations for equilibrium speciation of Ag(I) showed that for the $Ag_{<2nm}$ concentrations determined after one day in the

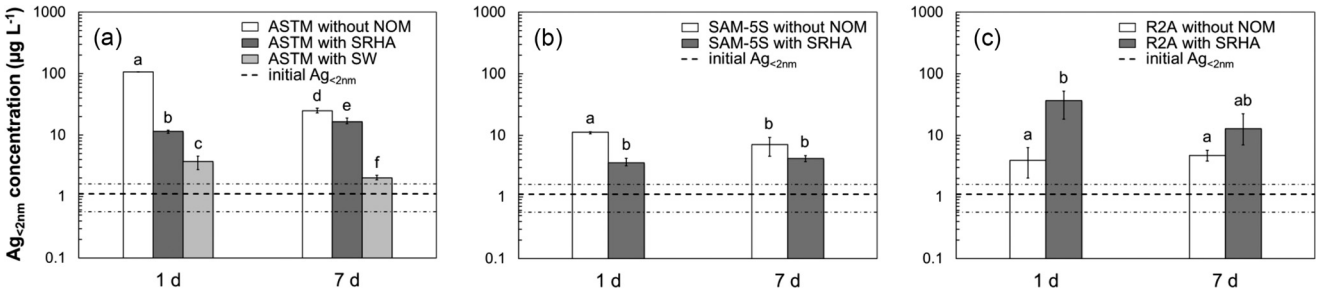

Fig. 1 Release of $Ag_{<2nm}$ from 30 nm Ag NPs (2 mg L^{-1}) in ASTM (a), SAM-5S (b), and R2A (c) medium with and without NOM for 1 d and 7 d exposure time. The error bars represent the minimal and maximal values of three replicates. The bold dashed lines correspond to the mean initial concentration of $Ag_{<2nm}$ from three replicates. The fine dash-dot lines correspond to the minimal and maximal values of the initial concentration of $Ag_{<2nm}$ from three replicates. Different letters denote statistically significant differences (p < 0.05, t-test). The data points with the same letters are not statistically different.

supernatant, the solution was undersaturated regarding solid phase silver chloride AgCl(s) and silver bromide AgBr(s) (Table S10‡). While in ASTM and R2A most of the Ag was present as Ag^+, aqueous silver chloride AgCl(aq) dominated in SAM-5S due to the highest Cl^- concentration. The $Ag_{<2nm}$ concentrations measured after one day in the supernatant of ASTM (105.6 ± 0.4 μg L^{-1}) and SAM-5S (11.2 ± 0.5 μg L^{-1}) were close to saturation concentrations calculated for ASTM (169 μg L^{-1}) regarding AgCl(s) and for SAM-5S (21 μg L^{-1}) regarding AgBr(s) (Table S11‡). This indicates that during dissolution of Ag NPs a part of released Ag^+ is likely transferred to AgCl(s) or AgBr(s), leading to the lower dissolved Ag concentration in SAM-5S compared to ASTM due to the lower solubility constant for AgBr(s).[55,56] In addition, the formation of surface precipitates of AgCl(s) and AgBr(s) as discussed below can hinder further dissolution of Ag NPs.

The low release of silver in the R2A medium, in turn, is likely explainable due to proteins or protein fragments present in the medium, which can form protein corona on the Ag NP surface[57,58] and hamper the diffusion and adsorption of oxidants as observed for citrate-coated Ag NPs in the presence of bovine serum albumin (BSA)[59] and luciferase.[57] Furthermore, the removal of potentially formed Ag^+–protein complexes by centrifugation, which cannot be fully excluded under the used centrifugation conditions, can result in underestimation of Ag^+ release. Interestingly, after 7 d of exposure time, the concentration of $Ag_{<2nm}$ decreased in ASTM (24.9 ± 2.2 μg L^{-1}) and SAM-5S (7.1 ± 2.4 μg L^{-1}) but not in R2A. This effect may be explained by the interplay of several processes like dissolution of the initial silver oxide layer, oxidation of the Ag NP surface, precipitation of AgCl(s), and re-sorption of released Ag^+ onto NP surfaces. After complete dissolution of the initial Ag_2O layer, the dissolution rate of Ag NP can be decreased since further dissolution is likely controlled by the oxidation reaction of the Ag NP surface.[16] The simultaneous formation of AgCl(s) precipitates can lead to decreasing concentration of $Ag_{<2nm}$ in the solution. Furthermore, the re-sorption of released Ag^+ onto the NP surface cannot be excluded,[28,60] which can be mediated by complexation sites provided by the free terminal carboxylate group of the citrate coating.[61] In contrast to ASTM and SAM-5S, no decrease in the concentration of $Ag_{<2nm}$ was observed in R2A after 7 d, which can be attributed to the absence of halide ions or to the above-mentioned protecting effect of sorbed proteins and their fragments.

The presence of NOM decreased $Ag_{<2nm}$ concentration in ASTM and SAM-5S. The decrease in ASTM was stronger for SW than for SRHA. The observed effect of NOM agrees well with the previously reported decrease in Ag^+ release with increasing concentrations of HA and fulvic acid (FA).[28] This effect can be explained by the physical protection of the Ag NP surface by adsorbed NOM[28,29] or by reduction of Ag^+ by NOM[62,63] and suggests a stronger protection by SW than SRHA. The stronger protection effect of SW may be explained by higher sorption of more hydrophilic[64] SW on the hydrophilic Ag NP surface compared to SRHA. In contrast, SRHA increased the $Ag_{<2nm}$ concentration in the R2A TM, which either suggests a weaker protection by NOM in this medium or a meaningfully larger active Ag NP surface[60] than in the other media. The latter is supported by the smallest Ag NP sizes and complete stabilization found in R2A relative to ASTM and SAM-5S (Fig. 2). Thus, the dissolution of Ag NP in TM seems to be controlled by the interplay of protecting mechanisms reducing the reactivity of the Ag NP surface and the stabilizing effects of NOM increasing the specific surface area of the Ag NPs. The higher release of silver from Ag NPs in all media by a factor of up to 2–100 compared to the original NP dispersions (Fig. 1) underlines the relevance of this process during ecotoxicological tests, especially in the light of the substantial toxicity induced by Ag^+.[29] The interplay between protecting and dissolution-supporting effects of organic constituents of the TM as well as NOM additives needs, however, more attention to uncover the underlying chemical processes and mechanisms.

Long term (≤7 d) aggregation of Ag NPs

In the absence of NOM, aggregation was observed in all TM, but not in deionized water (Fig. 2 and Fig. S2‡). Generally, the aggregation rates of the 100 nm Ag NPs were lower than those for 30 nm Ag NPs. This difference may result not only from the lower initial particle number concentration and lower collision probability of 100 nm Ag NPs compared to 30 nm Ag NPs, but also from differences in specific surfaces and thus NP reactivity towards aggregation cannot be excluded. This will be discussed on the basis of quantitative assessment of aggregation rates in the next section.

In the absence of NOM, Ag NP aggregation increased in the order R2A < SAM-5S < ASTM during the first day, whereas after seven days, Ag NP in SAM-5S showed a slightly higher hydrodynamic diameter than in ASTM. Nonetheless, these differences should be interpreted with care, since DLS analyses are biased in the presence of large aggregates. In ASTM and SAM-5S, the hydrodynamic diameter of both Ag NPs increased within the first day to 686–1025 nm and 460–1089 nm, respectively. In R2A the 30 nm NPs aggregated only within the first minutes to 65 nm and then remained nearly constant, whereas the aggregation of 100 nm Ag NPs was much slower and aggregate size increased slightly up to 185 nm within one day of exposure time (Fig. 2e and f and S2e and f‡). This effect can be explained again by the lower initial particle number concentration and lower collision probability of 100 nm Ag NPs compared to 30 nm Ag NPs.

Aggregation of Ag NPs was consistent with the colloidal stability that can be expected from the zeta potential, which was most negative in the R2A medium, although its absolute value was substantially reduced in all TM compared to deionized water (Fig. 2g and h). The latter is a direct consequence of electrical double layer compression at high ionic strength (>5 mmol L^{-1}).[50,51] Considering the respective ionic backgrounds in the different TM (Table S4‡) and the stability tendencies (Fig. 2), it is clear that additional processes are

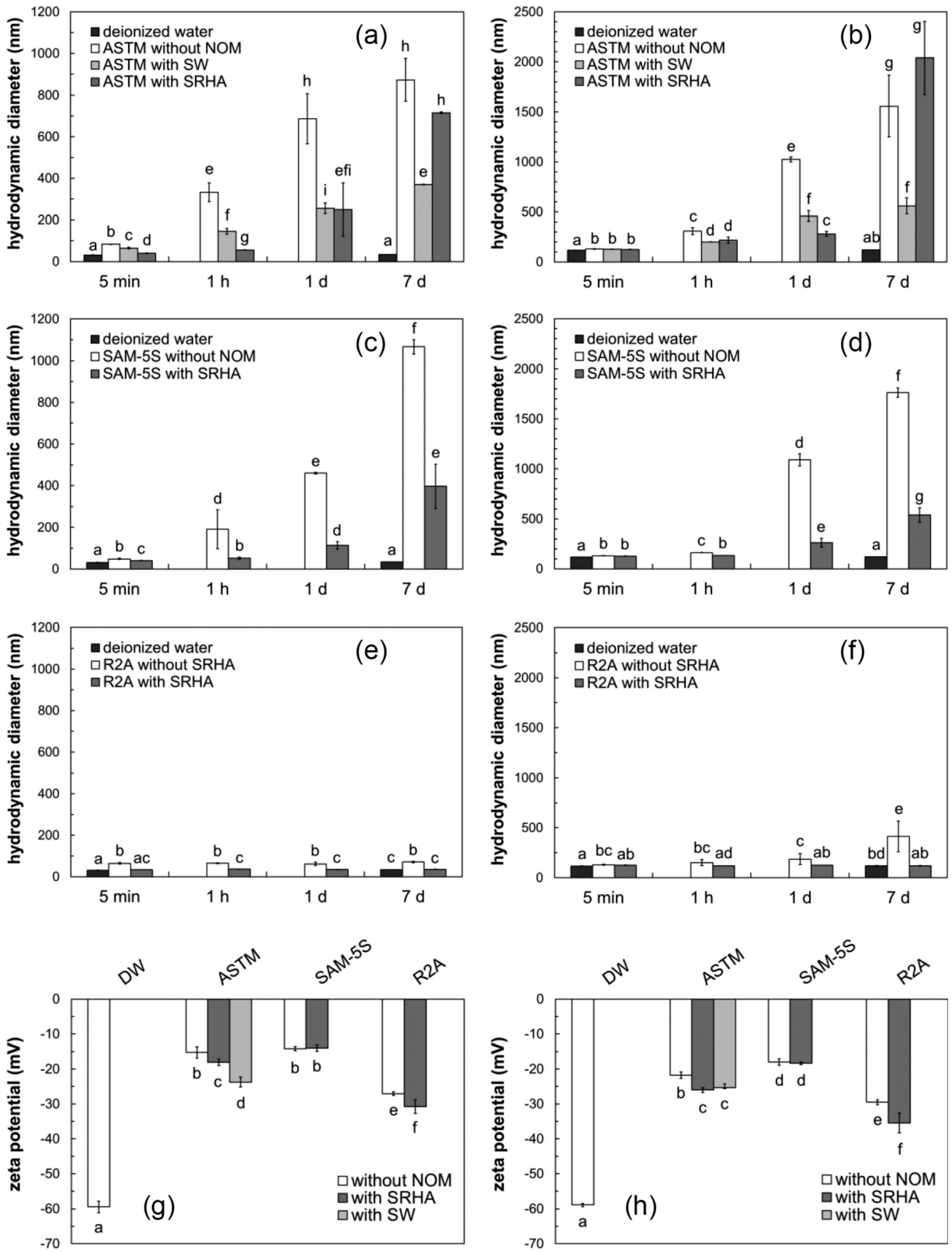

Fig. 2 Mean hydrodynamic diameter of 30 nm (a, c, e) and 100 nm (b, d, f) Ag NPs in ASTM (a, b), SAM-5S (c, d), and R2A (e, f) medium as a function of exposure time and mean zeta potential of 30 nm (g) and 100 nm (h) Ag NPs in deionized water (DW), ASTM, SAM-5S, and R2A medium in the absence as well as in the presence of NOM. Please consider the different *y* scales of (a), (c), and (e) with respect to (b), (d), and (f). Zeta potential was measured 5 min after adding Ag NPs to TM. The error bars represent minimal and maximal values of two replicates. Different letters denote statistically significant differences ($p < 0.05$, *t*-test). The data points with the same letters are not statistically different.

involved in the stabilization of Ag NPs. The medium R2A, which generated the most stable suspensions, contains among others the surfactant Tween 80. Tween 80 is known to readily adsorb onto the NP surface and stabilize NPs[60] – a process potentially of high relevance for the present study. Furthermore, the stabilizing effect of the proteins[65] which are also present in the R2A medium cannot be excluded.

NOM generally increased the stability of Ag NPs in all TM and at all points of time except for SRHA in ASTM in combination with 100 nm Ag NPs after 7 days (Fig. 2 and S2‡). These observations support the general expectation of electrosteric NP stabilization by NOM.[32–34] For exposure times exceeding one day SW served more efficiently as a stabilizing agent relative to SRHA (Fig. 2a and b), while for shorter exposure times, the stabilization by SRHA was slightly stronger or similar to that of SW. This could be explained by the different adsorption kinetics of SRHA and SW to Ag NPs or different aggregation mechanisms, which are further outlined below. However, neither SRHA nor SW completely prevented the Ag NPs in ASTM and SAM-5S from aggregation as the hydrodynamic diameter continuously increased during the seven days (Fig. 2c and d). In contrast to this, the addition of SRHA to R2A even completely prevented aggregation after one minute (Fig. 2e and f and S2e and f‡) likely due to the overlay of the stabilizing effects of SRHA and surfactant Tween 80.

Another interesting finding is that the zeta potential became slightly more negative after addition of NOM in ASTM and R2A, but not in SAM-5S (Fig. 2g and h). Although small, the differences range between 3 and 5 mV and are statistically significant. Thus, it cannot be excluded that these differences reflect changes in NP surface charge. Thus, NOM alone was not able to modify the zeta potential in the presence of inorganic constituents (SAM-5S), but it may have been able to increase its absolute value in the presence of additional organic compounds (R2A and ASTM). Although the final explanation requires more detailed investigations, the results suggest an interplay between NOM and further organic compounds present in ASTM and R2A or solid phase AgCl(s) precipitates, which were most likely present on the surface of Ag NPs in SAM-5S (see also discussion below).

If verified by further experiments, these findings demonstrate how the interplay between organic compounds and cations and its time dependence can affect dynamics in Ag NP stability. Therefore, using Ag NP pre-aged in TM likely results in different ecotoxicological effects relative to those used immediately after preparation, which was demonstrated for titanium dioxide NPs in ASTM medium.[1]

Early-stage aggregation kinetics of Ag NPs

The influence of particle number concentration on the initial aggregation rates of 30 nm and 100 nm Ag NPs in ASTM is presented in Fig. 3 on the basis of original aggregation data shown in Fig. S3.‡ The initial aggregation rates increased with increasing particle number concentration from 2.3 nm

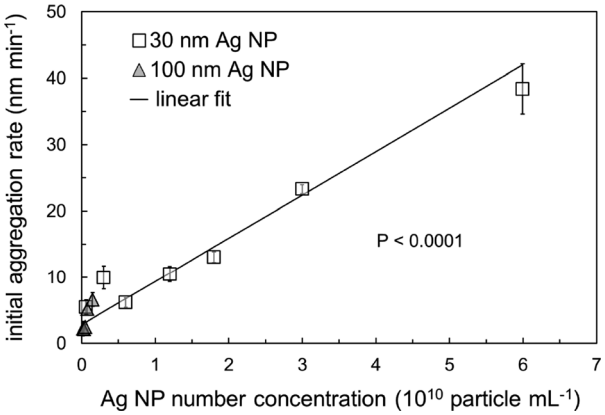

Fig. 3 Mean initial aggregation rate of 30 nm and 100 nm Ag NPs in ASTM medium as a function of particle number concentration. Mean values and standard deviations (error bars) were calculated from initial aggregation rates determined for the first 4, 5, and 6 min. Particle number concentration was calculated by the assumption that all particles are spherical and have the same particle diameter. The solid line represents the linear fit of combined experimental data for 30 nm and 100 nm Ag NPs.

min^{-1} (100 nm Ag NP) to 38 nm min^{-1} (30 nm Ag NP), and within the limits of data scattering, this dependence can be described with one linear function, suggesting comparable aggregation mechanisms for both particle sizes. Thus, no significant impacts of additional effects, such as specific surface or surface reactivity of the NPs, are evident from our data. The lower initial aggregation rates of 100 nm NPs compared to 30 nm NPs can thus be explained by the lower particle number concentration and thus the lower collision probability. The linear relationship between initial aggregation rate and particle concentration is also in a good agreement with the classical DLVO theory. A similar linear increase of the initial aggregation rate with increasing particle number concentration was also observed for 30 nm Ag NPs in Mg^{2+}-free R2A medium (Fig. S4‡).

Attachment efficiency profiles obtained for the 30 nm Ag NPs in the absence of NOM (Fig. 4) showed two aggregation regimes (*i.e.*, reaction and diffusion limited) and are in compliance with published literature.[17,18] The CCC values ranged from 1.6 ± 0.1 mmol L^{-1} (Ca^{2+} in ASTM) to 2.3 ± 0.1 mmol L^{-1} (Mg^{2+} in SAM-5S) and were by a factor of up to 1.2 higher for Mg^{2+} than for Ca^{2+} and by a factor of 1.2–1.4 higher for SAM-5S than for ASTM (Table 1).

The slightly lower CCC and, consequently, the higher efficiency of Ca^{2+} than Mg^{2+} to induce aggregation agrees well with the literature[14,18] and can be explained by stability constants of citrate complexes formed on the surface of the citrate-stabilized Ag NPs, which are higher with calcium ($\log K$ = 8.02 for $CaHC_6H_5O_7$, $\log K$ = 3.5 for $CaC_6H_5O_7^-$) than with magnesium ($\log K$ = 7.66 for $MgHC_6H_5O_7$, $\log K$ = 3.38 for $MgC_6H_5O_7^-$).[66]

On the other hand, the clearly higher CCC of Ca^{2+} and Mg^{2+} for SAM-5S than for ASTM despite comparable pH and

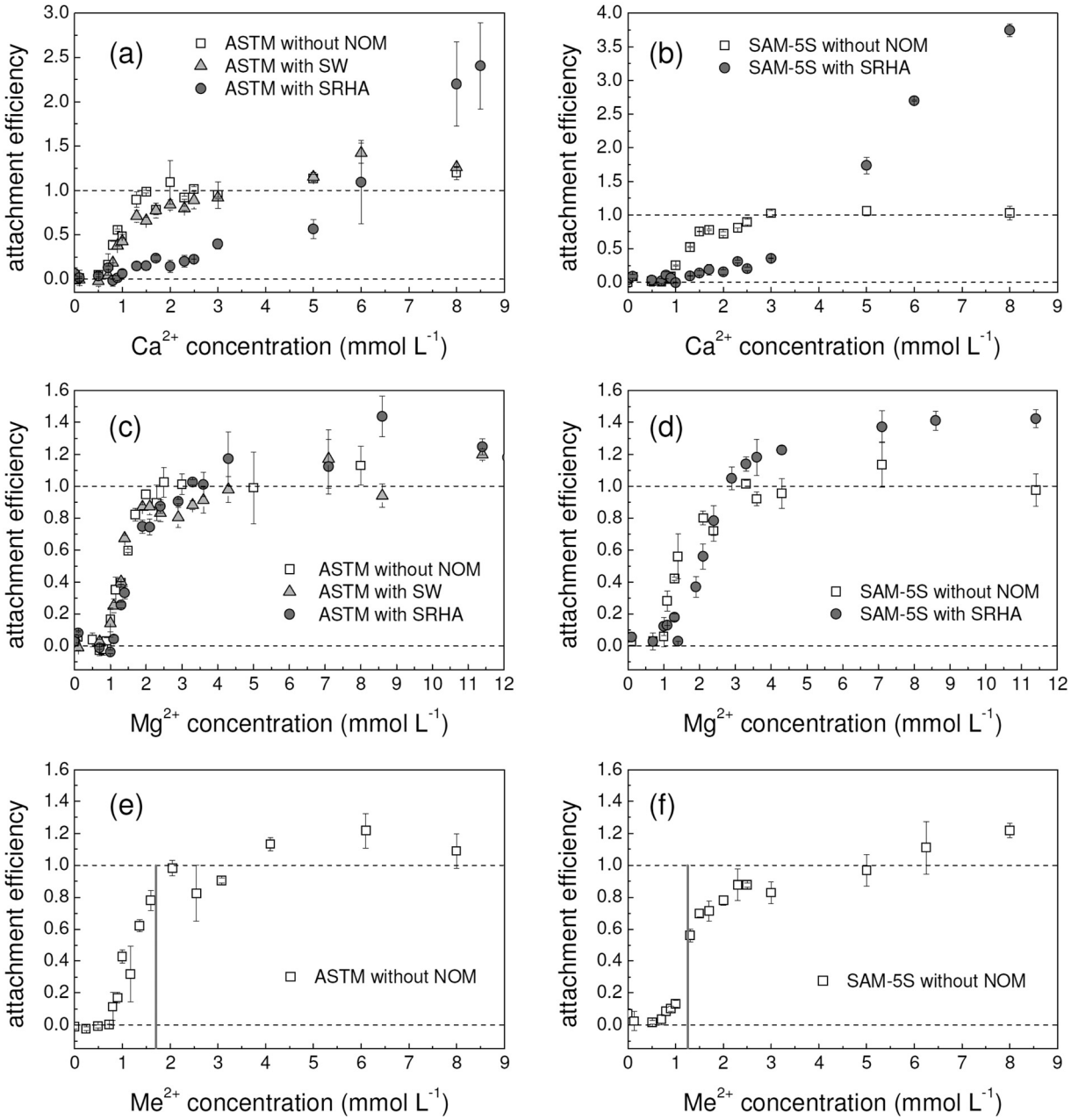

Fig. 4 Mean attachment efficiency profiles of 30 nm Ag NPs in cation-modified ASTM (a, c, e) and SAM-5S (b, d, f) medium in the absence as well as in the presence of NOM for Ca^{2+} (a, b), Mg^{2+} (c, d), and for mixtures of both Ca^{2+} and Mg^{2+} cations (e, f). The samples prepared for Ca^{2+} and Mg^{2+} addition did not contain Mg^{2+} and Ca^{2+}, respectively. The molar ratio of Ca^{2+} and Mg^{2+} was 0.7/1 for ASTM and 1/0.25 for SAM-5S medium. Me^{2+} concentration corresponds to the sum of Ca^{2+} and Mg^{2+} concentrations in the mixture. The grey vertical line shows the sum of Ca^{2+} and Mg^{2+} concentrations in the respective original medium. Horizontal dashed lines show the attachment efficiency values of 0 and 1. The values of $\alpha > 1$ indicate aggregation mechanisms not considered by the classical DLVO theory (*e.g.*, interparticle bridging by cation–NOM complexes). The error bars represent the minimal and maximal values of two replicates.

divalent cation concentrations indicate that in SAM-5S additional stabilization mechanisms are effective. Different concentrations of monovalent cations in the media cannot explain the differences in Ag NP stability since reported CCCs of monovalent cations for citrate-stabilized Ag NPs (48–122 mmol L^{-1})[14,18,67] are much higher than their concentration in the medium (2.43 mmol L^{-1} in ASTM and 1.06 mmol L^{-1} in SAM-5S, Table S4‡). Therefore, other TM constituents, namely, vitamins (present in ASTM) or halide ions (present in higher concentration in SAM-5S than in ASTM) are suspected to influence Ag NP stability.

Biotin (vitamin B_7), present in ASTM, for example, was found to form polymeric complexes through binding of Ag^+ to thioether and carbamide groups at concentrations of 2–25 mg L^{-1}.[55,56] Although biotin concentration in ASTM is much lower than these values, it cannot be excluded that such

Table 1 Mean CCC (in mmol L^{-1}) of 30 nm Ag NPs in ASTM, SAM-5S, and R2A medium in the absence as well as in the presence of NOM for Ca^{2+}, Mg^{2+} and for a mixture of both Ca^{2+} and Mg^{2+}

	ASTM	SAM-5S	R2A
Ca^{2+} (without NOM)	1.6 ± 0.1	2.2 ± 0.1	n.d.[b]
Ca^{2+} (with SRHA)	6.3 ± 1.4[a]	4.2 ± 0.1[a]	n.d.[b]
Ca^{2+} (with SW)	3.5 ± 0.1	n.d.[b]	n.d.[b]
Mg^{2+} (without NOM)	1.9 ± 0.1	2.3 ± 0.1	1.7 ± 0.2
Mg^{2+} (with SRHA)	3.4 ± 0.1	2.9 ± 0.1	3.6 ± 0.1
Mg^{2+} (with SW)	2.0 ± 0.1	n.d.[b]	n.d.[b]
Ca^{2+} + Mg^{2+} (without NOM)	2.0 ± 0.1	2.4 ± 0.1	n.d.[b]

[a] This concentration does not represent classical CCC, but marks the cation concentration at which α becomes larger than 1, indicating the concentration range where non-classical DLVO interaction mechanisms like aggregation by bridging become more important. [b] n.d.: not determined.

polymeric complexes are also formed on the Ag NP surface and support particle aggregation in ASTM. In order to test this hypothesis, we measured the initial aggregation rates of 30 nm Ag NPs in modified ASTM medium in the absence and presence of Ca^{2+} (0.7 mmol L^{-1}) as well as in the absence and presence of vitamins (B_1, B_7 and B_{12}) at different concentrations. The initial aggregation rate (*approx.* 2 nm min^{-1}) determined in the absence of vitamins did not change significantly in their presence even at 67–100-fold higher vitamin concentrations than present in typical ASTM medium (Fig. S5‡). This indicates that the vitamins used in ASTM medium do not influence the aggregation of Ag NP.

The concentration of Cl^- in SAM-5S medium is approximately 20-fold higher than in ASTM medium. Furthermore, SAM-5S medium contains Br^- ions, which are not present in ASTM medium. In order to evaluate the role of inorganic anions in the aggregation of Ag NPs, we performed early-stage aggregation experiments for 30 nm Ag NPs in deionized water as well as in modified ASTM medium in the absence and presence of $CaSO_4$, $CaCl_2$, $Ca(NO_3)_2$, or $CaBr_2$ at the same Ca^{2+} concentration (0.7 mmol L^{-1}). In deionized water as well as in modified ASTM medium no aggregation occurred in the presence of Cl^- or Br^- (Fig. 5a). In contrast to this, aggregation was observed in the presence of SO_4^{2-} or NO_3^- at the same Ca^{2+} concentration (Fig. 5a). Our results are, finally, in good agreement with those of El Badawy *et al.*,[12] who reported a much higher hydrodynamic diameter (determined by DLS) of Ag NPs in the presence of 10 mmol L^{-1} $NaNO_3$ than in the presence of the same amount of NaCl. In the solutions containing NaCl, no aggregation was observed even at low pH value (pH 3). El Badawy *et al.*[12] explained this effect by the high negative charge of AgCl(s) surface precipitates. The formation of solid phase AgCl(s) or AgBr(s) in our dispersions was confirmed by model calculations for the ASTM medium when modifying the anion composition by substitution of the $CaSO_4$ by $CaCl_2$ or $CaBr_2$ at equivalent Ca^{2+} concentration (0.7 mmol L^{-1}). The results of these calculations showed that 62.2% and 97.6% of the released silver was present as solid phase AgCl(s) and AgBr(s), respectively (Table S10‡). However, solid AgCl(s) precipitates or the presence of AgCl(s) colloids cannot easily explain a higher stability of Ag NPs in the TM. On the other hand, zeta potentials of Ag NPs measured in ASTM medium modified with $CaCl_2$ or $CaBr_2$ were slightly more negative than in ASTM medium with $Ca(NO_3)_2$ (Fig. 5b). Although these differences range only between 3 and 6 mV, they are statistically significant and they could support the idea that negatively charged surface precipitates of AgCl(s) or AgBr(s) may have stabilized nanoparticles in SAM-5S medium. Furthermore, the stabilization of nanoparticles by adsorption of Cl^- or Br^- cannot be excluded. The idea that halide ions stabilize the Ag NPs in the TM is further supported by the observation that the CCC for citrate-coated Ag NPs determined by Li *et al.*[13] was higher for NaCl (40

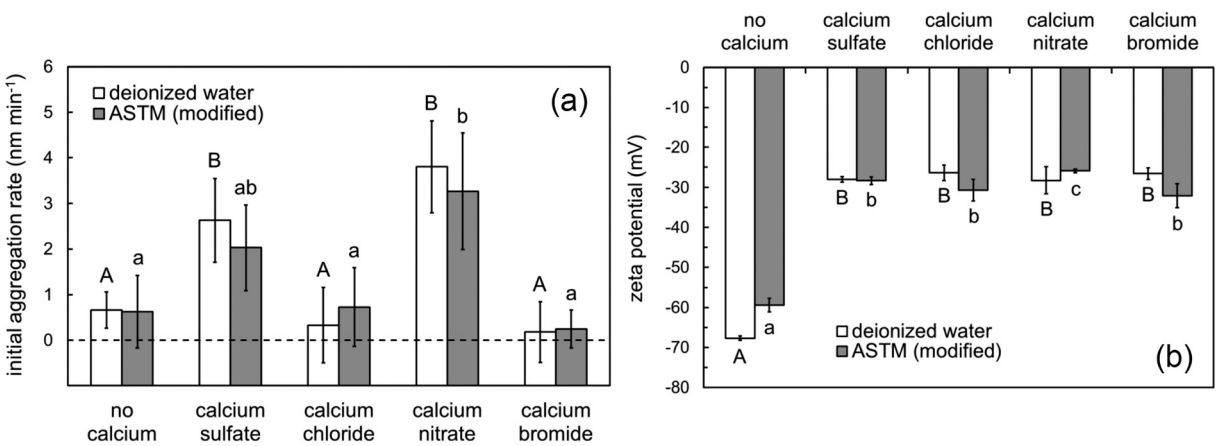

Fig. 5 Mean initial aggregation rates (a) and mean zeta potentials (b) of 30 nm Ag NPs in deionized water and modified ASTM medium in the absence and presence of $CaSO_4$, $CaCl_2$, $Ca(NO_3)_2$, or $CaBr_2$ at the same Ca^{2+} concentration (0.7 mmol L^{-1}). The modified ASTM medium did not contain Mg^{2+} and vitamins. The horizontal dashed line shows the initial aggregation rate when no aggregation occurs. The error bars represent the standard deviations from three replicates. Different letters denote statistically significant differences ($p < 0.05$, *t*-test) between the data points for deionized water (uppercase letters) and modified ASTM medium (lowercase letters). The data points with the same letters are not statistically different.

mmol L^{-1}) than for $NaNO_3$ (30 mmol L^{-1}). Furthermore, Tejamaya *et al.*[4] reported a reduction of absorbance and appearance of a shoulder at higher wavelengths in surface plasmon resonance spectra for citrate-coated Ag NPs after substitution of Cl^- by SO_4^{2-} or NO_3^- in 10-fold diluted OECD test medium, indicating, similar to our results, an increasing aggregation in the presence of SO_4^{2-} and NO_3^-. Partly opposite effects were reported in another study: Baalousha *et al.*[14] determined smaller CCCs for citrate-coated Ag NPs in NaCl than in Na_2SO_4 and $NaNO_3$ electrolyte by UV-vis measurements and explained this effect by increasing aggregation due to the possible bridging mechanisms by solid phase AgCl(s). In the presence of divalent cations (*i.e.*, Ca^{2+} and Mg^{2+}) the influence of anions was less distinct, especially for the experiments using the UV-vis method for the detection of the CCC of Ca^{2+} and Mg^{2+}. The CCC determined by DLS was slightly higher for $CaCl_2$ than for $CaSO_4$ and $Ca(NO_3)_2$ which is in compliance with the above discussed results. Most likely, whether or not the presence of Cl^- or Br^- stabilizes the Ag NPs depends on the concentrations of these anions and degree of dissolution of Ag NP. In order to clarify to which extent the aggregation state of Ag NPs depends on the concentrations of Cl^-, Br^-, and released Ag^+, further detailed investigations are needed.

Despite the high long-term stability of Ag NPs in R2A (Fig. 2), which is most probably due to the presence of surfactants, it is important to mention that the CCC of Mg^{2+} (1.7 ± 0.2 mmol L^{-1}) in R2A was even lower than in ASTM and SAM-5S in the absence of NOM (Table 1). Furthermore, even in the absence of Mg^{2+}, attachment efficiency α (0.15) was clearly above zero (Fig. 6), whereas the aggregation of Ag NPs in ASTM and SAM-5S media required Ca^{2+} or Mg^{2+} concentrations above 0.5–0.9 mmol L^{-1} (Fig. 4). One reason for these unexpected findings may be that the organic constituents of the R2A medium contain significant amounts of cations, which had not yet been considered. The total concentration of divalent (Ca^{2+} and Mg^{2+}) and monovalent (Na^+ and K^+) cations originating from the organic compounds of the R2A medium was 0.03 and 6.7 mmol L^{-1}, respectively (Table S12‡). Considering that K^+ (3.5 mmol L^{-1}) originated from K_2HPO_4, the total monovalent cation concentration in Mg^{2+}-free R2A medium was approximately 10 mmol L^{-1}. Additional experiments showed that aggregation of Ag NPs in deionized water in the presence of 0.03 mmol L^{-1} Ca^{2+} started at a Na^+ concentration of approximately 30 mmol L^{-1} (Fig. S6‡). Therefore, monovalent and divalent cations available in Mg^{2+}-free R2A medium alone cannot explain the increase in hydrodynamic diameter of Ag NPs. Most likely, this effect is induced by organic compounds present in R2A (amino acids, proteins and protein fragments; Table S4‡) despite the high stabilization efficiency of Tween 80. Additional aggregation experiments showed that in the absence of $MgSO_4$ the single organic constituents of R2A medium alone did not induce aggregation of Ag NPs (30 nm). Only the mixtures of individual organic compounds were able to initialize aggregation (Fig. S7‡). Most effective was the mixture of casein and yeast extract, which contain amino acids, proteins and protein fragments. Proteins adsorbing to Ag NP[57,59,68] can form a multilayer protein corona on NP surfaces,[57,58] which could also explain the fast initial increase in hydrodynamic diameter to 65 nm (Fig. 2) instead of aggregation. However, additional aggregation experiments in Mg^{2+}-free R2A at different Ag NP (30 nm) concentrations showed that particle size remained constant within 10 min, but it increased with increasing NP concentration (Fig. S4‡), such that even the initial increase in hydrodynamic diameter must be at least partly due to aggregation, which is in contrast to the assumption of the sole relevance of the protein corona. Which mechanisms induce the initial aggregation and whether or not the protein corona is also effective (or becomes effective only slowly, preventing further aggregation after some minutes) should be investigated in further detail by assessing the development and architecture of OM coatings in media with complex composition.

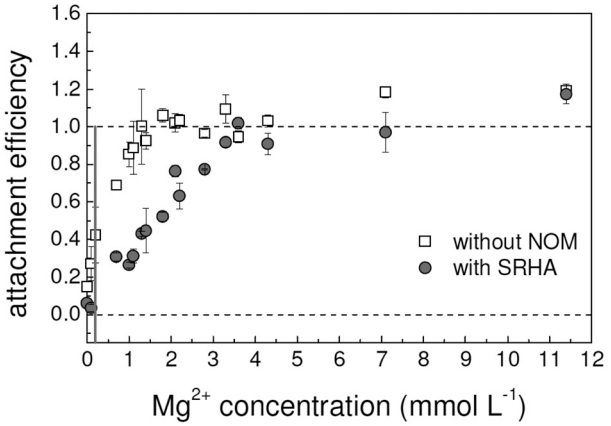

Fig. 6 Mean attachment efficiency profiles of 30 nm Ag NPs in cation modified R2A medium as a function of Mg^{2+} concentration. The grey vertical line shows the Mg^{2+} concentration in the original R2A medium. Horizontal dashed lines show the attachment efficiency values of 0 and 1. The error bars represent the minimal and maximal values of two replicates.

The attachment efficiency profiles for Me^{2+} used as Ca^{2+}–Mg^{2+} combinations at the Ca^{2+}/Mg^{2+} ratio of the respective media (Fig. 4e and f) indicated lower CCC of Me^{2+} in ASTM (2.0 ± 0.1 mmol L^{-1}) than in SAM-5S (2.4 ± 0.1 mmol L^{-1}). Thus, the media would have to be concentrated with respect to Me^{2+} concentration by a factor of only 1.2 for ASTM but of 2.0 for SAM-5S in order to reach the diffusion-limited regime.

This is in line with the findings for single cations. The total concentrations of divalent cations (Ca^{2+} + Mg^{2+} in ASTM and SAM-5S and Mg^{2+} in R2A) in all original TM (grey vertical lines in Fig. 4e and f and 6) lie in the reaction-limited regime, which predicts the formation of reaction-limited aggregates (RLAs) in the original TM. It is important to note that the Me^{2+} concentration in ASTM, but not in SAM-5S, is already close to the CCC, such that an overlay between diffusion and reaction control cannot be excluded in ASTM. In contrast to our observation for Ag NP, the results of Nur *et al.*[9] suggest

diffusion-limited aggregation for titanium dioxide NPs in several original TM. RLAs are usually more compact and stable compared to the diffusion-limited aggregates (DLAs).[69] The difference in aggregation regime between Ag NPs and titanium dioxide NPs thus suggests that organisms are confronted with different types of aggregates in the same test medium depending on the type of NP used.

Addition of NOM reduced α at the cation concentrations below the respective CCCs in all TM (Fig. 4), confirming the generally assumed stabilizing effect of NOM, which was stronger in the presence of Ca^{2+} than in the presence of Mg^{2+} (Table 1). This is in contrast to the strong destabilizing effect of Ca^{2+} on Ag NPs in the absence of NOM. Moreover, the stabilizing effect of SRHA in the presence of Ca^{2+} was dramatically stronger than that of SW, and the differences between Ca^{2+} and Mg^{2+} in the presence of NOM were lower for SW than for SRHA (Table 1 and Fig. 4). This can be a result of the stronger interaction between SRHA and Ca^{2+} than between SRHA and Mg^{2+}, assuming that the multivalent cations act as a bridging agent between Ag NPs and NOM coating. This is in line with the observation in Ca^{2+}-dominated systems, where the degree of SRHA-Me^{2+} interactions is higher compared to Mg^{2+}-dominated systems.[24,25]

In contrast to this, SRHA, but not SW, resulted in $\alpha > 1$ at Ca^{2+} concentrations above 6.3 ± 1.4 mmol L^{-1} for ASTM and above 4.2 ± 0.1 mmol L^{-1} for SAM-5S. Furthermore, α further increased with increasing Ca^{2+} concentration up to 2.2 ± 0.5 and 3.7 ± 0.1 mmol L^{-1} in ASTM and SAM-5S, respectively. Also, high Mg^{2+} concentrations resulted in increased α (1.4), but to a much lower extent than for Ca^{2+}. Such accelerated aggregation by SRHA in the presence of Ca^{2+} in high concentrations is in line with observations for Ag NPs[14,18] and Au NPs[24] in the presence of FA or HA and has been explained by bridging of NPs *via* Ca^{2+}–NOM complexes. The formation of NP aggregates by cation–NOM bridges is not consistent with the classical DLVO theory. Stankus *et al.*[24] reported that Mg^{2+} can enhance NP aggregation in the presence of SRHA (5 mg L^{-1} TOC), but to a lower extent than Ca^{2+}. The difference between Ca^{2+} and Mg^{2+} was explained by the larger hydration radius of Mg^{2+} compared to that of Ca^{2+}, leading to a lower tendency of Mg^{2+} to form inner sphere complexes with the NOM.[24] The fact that no effect was observed for Mg^{2+} in the work of Chen and Elimelech[25] is most likely a result of the significantly lower HA concentration (1 mg L^{-1} TOC) used in their work relative to the present study (9.4 mg L^{-1} TOC). This demonstrates that besides the concentration of divalent cations, the NOM concentration is a key parameter influencing bridging-determined aggregation.

The lack of aggregation enhancement by SW even in the presence of Ca^{2+} suggests that the SW constituents tend to undergo insignificant bridging with Ca^{2+} and Mg^{2+}, which is most probably due to differences in molecular weight, multifunctionality and affinity of functional groups towards Ca^{2+} and Mg^{2+}. While SW contains a large fraction of polysaccharides, phenolic and carboxylic functional groups are relevant in SRHA, suggesting that coordinative Me^{2+}–NOM interactions are more relevant in SRHA than in SW. In the presence of NOM, aggregation enhancement was also not observed in R2A medium, which underlines the reported strong stabilizing efficiency of Tween 80.[60] Furthermore, other organic constituents (proteins and protein fragments) of R2A may have modified the Ag NP surface and by this reduced the probability to form the Me^{2+}–NOM bridges between NPs.

Consequences for aggregation dynamics in test media

Summarizing the findings of this study, TM-specific changes in Ag NP aging and aggregation state as well as in the concentration and speciation of Ag(I) are suggested (Table 2). Regarding the nature of the aggregation process, both SAM-5S and ASTM seem to be similar, but differ in the expression of qualitative characteristics of NOM coating and aggregate size. In contrast, the R2A results in clearly smaller aggregates and Ag^+ concentrations than the other two TM. Thus, although the characteristics of the Ag NPs in R2A are not fully resolved, it seems unquestionable that they differ from those in the other two TM. Generally, under conditions of the investigated TM, the aggregation state of the Ag NPs is determined by the Ca^{2+}/Mg^{2+} ratio and concentration of halide ions in the TM (Table 2).

In all TM, reaction-limited aggregates are expected, with the consequence that their morphology and stability are sensitive to the TM composition and NP concentration. These aggregates are very small in R2A medium, such that their properties will differ strongly from those of ASTM and SAM-5S. Aggregate types and dynamics are expected to be comparable between ASTM and SAM-5S media, but zeta potential, aggregate sizes and NP reaction on the addition of different types of NOM and on the changes in concentration and composition of multivalent cations differ between these two media. Furthermore, the Me^{2+} concentration in ASTM is close to its CCC, suggesting the starting relevance of diffusion limitation for aggregation. These differences are mostly due to different initial molar ratios of Ca^{2+}/Mg^{2+} between the two media and the presence or absence of halide ions. In the absence of strong stabilizing agents like Tween 80, the most prominent differences among all TM are the concentration of Cl^- and the dominance of Ca^{2+}.

With respect to the inorganic constituents relevant for Ag NP dissolution, surface reaction and aggregation, the composition of the SAM-5S resembles that of the Rhine water discussed by Metreveli *et al.*[23] and suggests that Ag NP aggregates are at least partly stabilized in the presence of Cl^-, but with a distinct speciation of Ag(I) in this water. More generally speaking, our results suggest that Ag NPs may be only incompletely stabilized by NOM and halides in natural waters, and NOM quality in addition to ion composition will strongly affect the nature of the aggregates forming. Thus, as long as NOM in natural water is similar to SW, bridging-determined aggregates in that water will have low relevance compared to waters rich in NOM similar to SRHA.

Table 2 Overview on NP characteristics in TM and their dynamics and changes upon modification of TM composition as suggested from this study

	ASTM	SAM-5S	R2A
Salt composition			
Ca^{2+}/Mg^{2+} [a]	0.69/1	1/0.25	0/0.2
Cl^-/Br^- [a]	0.11/0	2.05/0.01	0/0
Formation of Ag(I) species			
Ag^+ concentration	++++	++	+
Predominant Ag(I) species	Ag^+	AgCl(aq)	Ag^+; Ag^+–protein complexes?
Impact of NOM	NOM reduces Ag^+ SW > SRHA	SRHA reduces Ag^+	SRHA increases Ag^+
Aggregation and colloidal stability			
Tendency to aggregate	++++	+++	+
$CCC(Mg^{2+})/CCC(Ca^{2+})$ [a]	1.9/1.6	2.3/2.2	1.7/n.d. [b]
NP stabilization	No effect of vitamins	By halide surface precipitates?	By Tween 80, protein corona?
Impact of NOM in original TM (at low Me^{2+} concentrations)	Electrosteric stabilization SW ≤ SRHA (short term) SW > SRHA (long term)	Electrosteric stabilization	Electrosteric stabilization
Effect of Me^{2+} in the presence of NOM	Ca^{2+} enhances electrosteric stabilization compared to Mg^{2+} SRHA > SW		
	Me^{2+} induces bridging-determined aggregation at high concentrations:		No bridging-determined aggregation
	Ca^{2+}: >6.3 mmol L^{-1}	Ca^{2+}: >4.2 mmol L^{-1}	
	Mg^{2+}: >3.4 mmol L^{-1}	Mg^{2+}: >2.9 mmol L^{-1}	
General strength of cation effects	$Ca^{2+} > Mg^{2+}$ based on Me^{2+}–citrate and Me^{2+}–NOM interactions		
Expected characteristics relevant for ecotoxicological potential of Ag NP			
Dissolved species	++++ (Ag^+)	+++ (Ag^+; AgCl(aq))	+ (Ag^+)
NP surface	Ag–citrate	AgCl(s)	Ag–protein?
Effectiveness of NOM coating	+++	+++++	+
Aggregate size	++++	++++	+
Aggregate type	Reaction-limited aggregates Overlay with diffusion limitation		Reaction-limited aggregates small clusters?
Dynamic aggregation properties within test duration	Aggregate size increases with time. Size and morphology strongly affected by NP concentration and solution chemistry		Aggregate size constant but depends on NP concentration
NOM-bridged aggregates	Low relevance but expected relevance in hard water		
Impacts of changes in TM composition			
Addition of Cl^-	Stabilizes NP, AgCl(s) on NP surface	Enhances aggregation by AgCl(s) bridging?	AgCl(s) on NP surface?
Reduction in Ca^{2+}/Mg^{2+} ratio	Reduces aggregate size and stabilizing effect of SRHA coating		
Modifying NOM composition	SW: coating based on NOM–Ag interactions SRHA: coating based on Ca^{2+}–NOM interactions		Effects overbalanced by Tween 80 effect?

[a] In mmol L^{-1}/mmol L^{-1}. [b] n.d.: not determined.

Conclusions

In summary, not only the composition of the TM but also the Ag NP concentration and the duration of the ecotoxicological and biological studies will significantly affect the aggregation status of Ag NPs. This underlines the requirement to carefully interpret dose–response relationships and differences in toxicity towards the same organisms, which have been obtained for TM with different composition. In the absence of NOM, the formation of aggregates is controlled by the molar ratio of multivalent cations and by the type of anions. Under the conditions of TM, the formation of bridging-determined aggregates induced by NOM is not relevant but could increase in relevance in natural surface waters with a high concentration of cations. Pre-aging of NP in the TM prior to the biological and ecotoxicological studies will minimize the time-dependent transformations and changes in colloidal state and concentration of NPs during the tests and will allow the investigation not only of the effect of different states of aggregation and different coating structures but also of different concentrations of metal cations released from NPs in the medium under conditions comparable with realistic environmental scenarios.

The results of our study do not only show that by using different TM, the same Ag NPs will likely have different ecotoxicological potentials, but they also open perspectives for targeted research on the impact of individual Ag NP species on ecotoxicological potential. For example, increasing the Ca^{2+}/Mg^{2+} concentration ratio in the absence of NOM will enhance aggregation. By modifying the nature of the NOM

additive of the TM and the ratio between Ca^{2+} and Mg^{2+}, the effectiveness of the electrosteric stabilization by NOM will be modified and bridging-determined aggregation may be induced. The use of SW and the dominance of Mg^{2+} will favor aggregates formed on the basis of extended DLVO interactions. In ecotoxicological tests, these composition parameters could be adjusted within ranges where no or low effects on the vitality of test organisms are expected in order to obtain Ag NPs with different coating stability, surface and aggregate characteristics, and concentration of dissolved Ag(I) species. It is furthermore essential to know how ecotoxicity results obtained in conventional TM could be transferred to environmental systems, the composition of which differs often significantly from that of the TM with the consequence of different aggregation properties.[6] Taking advantage of the knowledge of NP transformations in TM with modified chemical composition will, therefore, allow the prediction of specific NP characteristics and aggregation states in natural environmental systems, which may help in a second step to extrapolate ecotoxicological findings to the field.

Acknowledgements

The authors thank the German Research Foundation (DFG) for financial support within research unit INTERNANO (FOR 1536 "Mobility, aging and functioning of engineered inorganic nanoparticles at the aquatic–terrestrial interface"), subprojects SCHA849/16, SCHU2271/5 and MA3273/3. We thank Bärbel Schmidt for her contribution to the aggregation and silver release experiments. We are also grateful to Dr. Wolfgang Fey for the ICP-MS measurements.

References

1 F. Seitz, S. Lüderwald, R. R. Rosenfeldt, R. Schulz and M. Bundschuh, Aging of TiO_2 nanoparticles transiently increases their toxicity to the pelagic microcrustacean *Daphnia magna*, *Plos One*, 2015, **10**(5), e0126021.

2 I. Romer, T. A. White, M. Baalousha, K. Chipman, M. R. Viant and J. R. Lead, Aggregation and dispersion of silver nanoparticles in exposure media for aquatic toxicity tests, *J. Chromatogr. A*, 2011, **1218**(27), 4226–4233.

3 I. Romer, A. J. Gavin, T. A. White, R. C. Merrifield, J. K. Chipman, M. R. Viant and J. R. Lead, The critical importance of defined media conditions in *Daphnia magna* nanotoxicity studies, *Toxicol. Lett.*, 2013, **223**(1), 103–108.

4 M. Tejamaya, I. Romer, R. C. Merrifield and J. R. Lead, Stability of citrate, PVP, and PEG coated silver nanoparticles in ecotoxicology media, *Environ. Sci. Technol.*, 2012, **46**(13), 7011–7017.

5 C. M. Zhao and W. X. Wang, Size-dependent uptake of silver nanoparticles in *Daphnia magna*, *Environ. Sci. Technol.*, 2012, **46**(20), 11345–11351.

6 S. Park, J. Woodhall, G. B. Ma, J. G. C. Veinot, M. S. Cresser and A. B. A. Boxall, Regulatory ecotoxicity testing of engineered nanoparticles: Are the results relevant to the natural environment?, *Nanotoxicology*, 2014, **8**(5), 583–592.

7 K. Wiench, W. Wohlleben, V. Hisgen, K. Radke, E. Salinas, S. Zok and R. Landsiedel, Acute and chronic effects of nano- and non-nano-scale TiO_2 and ZnO particles on mobility and reproduction of the freshwater invertebrate *Daphnia magna*, *Chemosphere*, 2009, **76**(10), 1356–1365.

8 A. M. Horst, Z. X. Ji and P. A. Holden, Nanoparticle dispersion in environmentally relevant culture media: A TiO_2 case study and considerations for a general approach, *J. Nanopart. Res.*, 2012, **14**(8), 1014.

9 Y. Nur, J. R. Lead and M. Baalousha, Evaluation of charge and agglomeration behavior of TiO_2 nanoparticles in ecotoxicological media, *Sci. Total Environ.*, 2015, **535**, 45–53 (Special Issue: Engineered nanoparticles in soils and waters).

10 M. Vielkind, I. Kampen and A. Kwade, Zinc oxide nanoparticles in bacterial growth medium: Optimized dispersion and growth inhibition of *Pseudomonas putida*, *Adv. Nanopart.*, 2013, **2**, 287–293.

11 R. Tantra, S. H. Jing, S. K. Pichaimuthu, N. Walker, J. Noble and V. A. Hackley, Dispersion stability of nanoparticles in ecotoxicological investigations: The need for adequate measurement tools, *J. Nanopart. Res.*, 2011, **13**(9), 3765–3780.

12 A. M. El Badawy, T. P. Luxton, R. G. Silva, K. G. Scheckel, M. T. Suidan and T. M. Tolaymat, Impact of environmental conditions (pH, ionic strength, and electrolyte type) on the surface charge and aggregation of silver nanoparticles suspensions, *Environ. Sci. Technol.*, 2010, **44**(4), 1260–1266.

13 X. Li, J. J. Lenhart and H. W. Walker, Aggregation kinetics and dissolution of coated silver nanoparticles, *Langmuir*, 2012, **28**(2), 1095–1104.

14 M. Baalousha, Y. Nur, I. Romer, M. Tejamaya and J. R. Lead, Effect of monovalent and divalent cations, anions and fulvic acid on aggregation of citrate-coated silver nanoparticles, *Sci. Total Environ.*, 2013, **454**, 119–131.

15 C. Levard, E. M. Hotze, B. P. Colman, A. L. Dale, L. Truong, X. Y. Yang, A. J. Bone, G. E. Brown, R. L. Tanguay, R. T. Di Giulio, E. S. Bernhardt, J. N. Meyer, M. R. Wiesner and G. V. Lowry, Sulfidation of silver nanoparticles: Natural Antidote to their toxicity, *Environ. Sci. Technol.*, 2013, **47**(23), 13440–13448.

16 C. Levard, S. Mitra, T. Yang, A. D. Jew, A. R. Badireddy, G. V. Lowry and G. E. Brown, Effect of chloride on the dissolution rate of silver nanoparticles and toxicity to *E. coli*, *Environ. Sci. Technol.*, 2013, **47**(11), 5738–5745.

17 K. L. Chen and M. Elimelech, Aggregation and deposition kinetics of fullerene (C_{60}) nanoparticles, *Langmuir*, 2006, **22**(26), 10994–11001.

18 K. A. Huynh and K. L. Chen, Aggregation kinetics of citrate and polyvinylpyrrolidone coated silver nanoparticles in monovalent and divalent electrolyte solutions, *Environ. Sci. Technol.*, 2011, **45**(13), 5564–5571.

19 E. Topuz, L. Sigg and I. Talinli, A systematic evaluation of agglomeration of Ag and TiO_2 nanoparticles under freshwater relevant conditions, *Environ. Pollut.*, 2014, **193**, 37–44.

20 E. Topuz, J. Traber, L. Sigg and I. Talinli, Agglomeration of Ag and TiO_2 nanoparticles in surface and wastewater: Role of calcium ions and of organic carbon fractions, *Environ. Pollut.*, 2015, **204**, 313–323.

21 S. Hall, T. Bradley, J. T. Moore, T. Kuykindall and L. Minella, Acute and chronic toxicity of nano-scale TiO_2 particles to freshwater fish, cladocerans, and green algae, and effects of organic and inorganic substrate on TiO_2 toxicity, *Nanotoxicology*, 2009, **3**(2), 91–97.

22 A. Philippe and G. E. Schaumann, Interactions of dissolved organic matter with artificial inorganic colloids: A review, *Environ. Sci. Technol.*, 2014, **48**(16), 8946–8962.

23 G. Metreveli, A. Philippe and G. E. Schaumann, Disaggregation of silver nanoparticle homoaggregates in a river water matrix, *Sci. Total Environ.*, 2015, **535**, 35–44 (Special Issue: Engineered nanoparticles in soils and waters).

24 D. P. Stankus, S. E. Lohse, J. E. Hutchison and J. A. Nason, Interactions between natural organic matter and gold nanoparticles stabilized with different organic capping agents, *Environ. Sci. Technol.*, 2011, **45**(8), 3238–3244.

25 K. L. Chen and M. Elimelech, Influence of humic acid on the aggregation kinetics of fullerene (C_{60}) nanoparticles in monovalent and divalent electrolyte solutions, *J. Colloid Interface Sci.*, 2007, **309**(1), 126–134.

26 S. Klitzke, G. Metreveli, A. Peters, G. E. Schaumann and F. Lang, The fate of silver nanoparticles in soil solution - Sorption of solutes and aggregation, *Sci. Total Environ.*, 2015, **535**, 54–60 (Special Issue: Engineered nanoparticles in soils and waters).

27 O. Furman, S. Usenko and B. L. T. Lau, Relative importance of the humic and fulvic fractions of natural organic matter in the aggregation and deposition of silver nanoparticles, *Environ. Sci. Technol.*, 2013, **47**(3), 1349–1356.

28 J. Y. Liu and R. H. Hurt, Ion release kinetics and particle persistence in aqueous nano-silver colloids, *Environ. Sci. Technol.*, 2010, **44**(6), 2169–2175.

29 K. M. Newton, H. L. Puppala, C. L. Kitchens, V. L. Colvin and S. J. Klaine, Silver nanoparticle toxicity to *Daphnia magna* is a function of dissolved silver concentration, *Environ. Toxicol. Chem.*, 2013, **32**(10), 2356–2364.

30 M. A. Chappell, L. F. Miller, A. J. George, B. A. Pettway, C. L. Price, B. E. Porter, A. J. Bednar, J. M. Seiter, A. J. Kennedy and J. A. Steevens, Simultaneous dispersion-dissolution behavior of concentrated silver nanoparticle suspensions in the presence of model organic solutes, *Chemosphere*, 2011, **84**(8), 1108–1116.

31 F. Seitz, R. R. Rosenfeldt, K. Storm, G. Metreveli, G. E. Schaumann, R. Schulz and M. Bundschuh, Effects of silver nanoparticle properties, media pH and dissolved organic matter on toxicity to *Daphnia magna*, *Ecotoxicol. Environ. Saf.*, 2015, **111**, 263–270.

32 R. Kretzschmar, H. Holthoff and H. Sticher, Influence of pH and humic acid on coagulation kinetics of kaolinite: A dynamic light scattering study, *J. Colloid Interface Sci.*, 1998, **202**(1), 95–103.

33 M. Baalousha, Aggregation and disaggregation of iron oxide nanoparticles: influence of particle concentration, pH and natural organic matter, *Sci. Total Environ.*, 2009, **407**(6), 2093–2101.

34 J. F. Liu, S. Legros, G. B. Ma, J. G. C. Veinot, F. von der Kammer and T. Hofmann, Influence of surface functionalization and particle size on the aggregation kinetics of engineered nanoparticles, *Chemosphere*, 2012, **87**(8), 918–924.

35 P. Das, M. A. Xenopoulos and C. D. Metcalfe, Toxicity of silver and titanium dioxide nanoparticle suspensions to the aquatic invertebrate, *Daphnia magna*, *Bull. Environ. Contam. Toxicol.*, 2013, **91**(1), 76–82.

36 S. B. Lovern and R. Klaper, *Daphnia magna* mortality when exposed to titanium dioxide and fullerene (C_{60}) nanoparticles, *Environ. Toxicol. Chem.*, 2006, **25**(4), 1132–1137.

37 F. Seitz, M. Bundschuh, R. R. Rosenfeldt and R. Schulz, Nanoparticle toxicity in *Daphnia magna* reproduction studies: The importance of test design, *Aquat. Toxicol.*, 2013, **126**, 163–168.

38 J. Turkevich, P. C. Stevenson and J. Hillier, A study of the nucleation and growth processes in the synthesis of colloidal gold, *Discuss. Faraday Soc.*, 1951, **11**, 55–75.

39 N. Schultz, G. Metreveli, M. Franzreb, F. H. Frimmel and C. Syldatk, Zeta potential measurement as a diagnostic tool in enzyme immobilisation, *Colloids Surf., B*, 2008, **66**(1), 39–44.

40 *ASTM Standard E729. Standard guide for conducting acute toxicity tests on test materials with fishes, macroinvertebrates, and amphibian*, 2007.

41 F. Seitz, R. R. Rosenfeldt, S. Schneider, R. Schulz and M. Bundschuh, Size-, surface- and crystalline structure composition-related effects of titanium dioxide nanoparticles during their aquatic life cycle, *Sci. Total Environ.*, 2014, **493**, 891–897.

42 U. Borgmann, V. Cheam, W. P. Norwood and J. Lechner, Toxicity and bioaccumulation of thallium in *Hyalella azteca*, with comparison to other metals and prediction of environmental impact, *Environ. Pollut.*, 1998, **99**(1), 105–114.

43 R. R. Rosenfeldt, F. Seitz, R. Schulz and M. Bundschuh, Heavy metal uptake and toxicity in the presence of titanium dioxide nanoparticles: A factorial approach using *Daphnia magna*, *Environ. Sci. Technol.*, 2014, **48**(12), 6965–6972.

44 C. Loureiro, B. B. Castro, J. L. Pereira and F. Goncalves, Performance of standard media in toxicological assessments with *Daphnia magna*: Chelators and ionic composition versus metal toxicity, *Ecotoxicology*, 2011, **20**(1), 139–148.

45 F. Namvar, H. S. Rahman, R. Mohamad, J. Baharara, M. Mahdavi, E. Amini, M. S. Chartrand and S. K. Yeap, Cytotoxic effect of magnetic iron oxide nanoparticles synthesized via seaweed aqueous extract, *Int. J. Nanomed.*, 2014, **9**, 2479–2488.

46 J. Buffle, K. J. Wilkinson, S. Stoll, M. Filella and J. Zhang, A Generalized description of aquatic colloidal interactions: The three-colloidal component-approch, *Environ. Sci. Technol.*, 1998, **32**(19), 2887–2899.

47 J. G. Hering and F. M. M. Morel, Humic acid complexation of calcium and copper, *Environ. Sci. Technol.*, 1988, **22**(10), 1234–1237.
48 J. P. Gustafsson, *Visual MINTEQ, version 3.0*, (last visited: June 20, 2015), http://vminteq.lwr.kth.se/.
49 M. Bundschuh, J. P. Zubrod, D. Englert, F. Seitz, R. R. Rosenfeldt and R. Schulz, Effects of nano-TiO_2 in combination with ambient UV-irradiation on a leaf shredding amphipod, *Chemosphere*, 2011, **85**(10), 1563–1567.
50 B. V. Derjaguin and L. Landau, Theory of stability of highly charged lyophobic sols and adhesion of highly charged particles in solutions of electrolytes, *Acta Physicochim. URSS*, 1941, **14**, 633–662.
51 E. J. W. Verwey and J. T. G. Overbeek, *Theory of Stability of Lyophobic Colloids*, Elsevier, Amsterdam, 1948.
52 M. Hassellov, J. W. Readman, J. F. Ranville and K. Tiede, Nanoparticle analysis and characterization methodologies in environmental risk assessment of engineered nanoparticles, *Ecotoxicology*, 2008, **17**(5), 344–361.
53 R. Finsy, Particle sizing by quasi-elastic light scattering, *Adv. Colloid Interface Sci.*, 1994, **52**, 79–143.
54 M. Y. Lin, H. M. Lindsay, D. A. Weitz, R. Klein, R. C. Ball and P. Meakin, Universal diffusion-limited colloid aggregation, *J. Phys.: Condens. Matter*, 1990, **2**(13), 3093–3113.
55 K. Aoki and W. Saenger, Interactions of biotin with metal ions. X-ray crystal structure of the polymeric biotin-silver(I) nitrate complex: Metal bonding to thioether and ureido carbonyl groups, *J. Inorg. Biochem.*, 1983, **19**(3), 269–273.
56 I. Goncharova, D. Sykora and M. Urbanova, Association of biotin with silver (I) in solution: A circular dichroism study, *Tetrahedron: Asymmetry*, 2010, **21**(15), 1916–1920.
57 A. Kakinen, F. Ding, P. Y. Chen, M. Mortimer, A. Kahru and P. C. Ke, Interaction of firefly luciferase and silver nanoparticles and its impact on enzyme activity, *Nanotechnology*, 2013, **24**(34), 345101.
58 R. Chen, P. Choudhary, R. N. Schurr, P. Bhattacharya, J. M. Brown and P. C. Ke, Interaction of lipid vesicle with silver nanoparticle-serum albumin protein corona, *Appl. Phys. Lett.*, 2012, **100**(1), 013703.
59 A. K. Ostermeyer, C. K. Mumuper, L. Semprini and T. Radniecki, Influence of bovine serum albumin and alginate on silver nanoparticle dissolution and toxicity to *Nitrosomonas europaea*, *Environ. Sci. Technol.*, 2013, **47**(24), 14403–14410.
60 X. Li and J. J. Lenhart, Aggregation and dissolution of silver nanoparticles in natural surface water, *Environ. Sci. Technol.*, 2012, **46**(10), 5378–5386.
61 C. H. Munro, W. E. Smith, M. Garner, J. Clarkson and P. C. White, Characterization of the surface of a citrate-reduced colloid optimized for use as a substrate for surface-enhanced resonance Raman-scattering, *Langmuir*, 1995, **11**(10), 3712–3720.
62 N. Akaighe, R. I. MacCuspie, D. A. Navarro, D. S. Aga, S. Banerjee, M. Sohn and V. K. Sharma, Humic acid-induced silver nanoparticle formation under environmentally relevant conditions, *Environ. Sci. Technol.*, 2011, **45**(9), 3895–3901.
63 N. F. Adegboyega, V. K. Sharma, K. Siskova, R. Zboril, M. Sohn, B. J. Schultz and S. Banerjee, Interactions of aqueous Ag^+ with fulvic acids: Mechanisms of silver nanoparticle formation and investigation of stability, *Environ. Sci. Technol.*, 2013, **47**(2), 757–764.
64 R. R. Rosenfeldt, F. Seitz, L. Senn, C. Schilde, R. Schulz and M. Bundschuh, Nanosized titanium dioxide reduces copper toxicity - The role of organic material and the crystalline phase, *Environ. Sci. Technol.*, 2015, **49**(3), 1815–1822.
65 J. T. Tai, C. S. Lai, H. C. Ho, Y. S. Yeh, H. F. Wang, R. M. Ho and D. H. Tsai, Protein silver nanoparticle interactions to colloidal stability in acidic environments, *Langmuir*, 2014, **30**(43), 12755–12764.
66 T. B. Field, J. Coburn, J. L. McCourt and W. A. E. McBryde, Composition and stability of some metal citrate and diglycolate complexes in aqueous solution, *Anal. Chim. Acta*, 1975, **74**(1), 101–106.
67 A. M. El Badawy, K. G. Scheckel, M. Suidan and T. Tolaymat, The impact of stabilization mechanism on the aggregation kinetics of silver nanoparticles, *Sci. Total Environ.*, 2012, **429**, 325–331.
68 Y. Wang and Y. N. Ni, New insight into protein-nanomaterial interactions with UV-visible spectroscopy and chemometrics: Human serum albumin and silver nanoparticles, *Analyst (Cambridge, U. K.)*, 2014, **139**(2), 416–424.
69 P. Meakin, Models for colloidal aggregation, *Annu. Rev. Phys. Chem.*, 1988, **39**(1), 237–267.